View metadata, citation and similar papers at core.ac.uk
brought to you by CORE
provided by E-resource repository of the University of Latvia

J. Cryst. Growth 459 (2017) 100-104.

Synthesis and characterization of ZnO/ZnS/MoS_2 core-shell nanowires

Edgars Butanovs[1], Alexei Kuzmin[1], Jelena Butikova[1], Sergei Vlassov[2], Boris Polyakov[1*]

[1]Institute of Solid State Physics, University of Latvia, Kengaraga street 8, LV-1063 Riga, Latvia

[2]Institute of Physics, University of Tartu, Ravila 14c, 50412 Tartu, Estonia

*e-mail: boris.polyakov@cfi.lu.lv

Abstract

Hybrid nanostructures composed of layered materials have recently attracted a lot of attention due to their promising electronic and catalytic properties. In this study, we describe a novel synthesis strategy of ZnO/ZnS/MoS_2 core-shell nanowire growth using a three-step route. First, ZnO nanowire array was grown on a silicon wafer. Second, the sample was immersed in ammonium molybdate solution and dried. At the third step, the sample was annealed in a sulfur atmosphere at 700 ºC. Two solid state chemical reactions occur simultaneously during the annealing and result in a formation of ZnS and MoS_2 phases. Produced ZnO/ZnS/MoS_2 core-shell nanowires were characterized by scanning and transmission electron microscopy, whereas their chemical composition was confirmed by selected area electron diffraction and micro-Raman spectroscopy.

Keywords:

A1 Characterization; A1 Crystal morphology; A1 Nanostructures; B1 Oxides; B1 Sulfides; B1 Zinc compounds.

1. Introduction.

Recent advances in research of layered materials, as for example, graphene, have stimulated studies of two-dimensional (2D) transition metal dichalcogenides (TMDs) with unique properties that do not exist in their bulk counterparts [1, 2]. TMDs, such as MS_2 (M = W, Mo), are indirect bandgap semiconductors in bulk form, however, when scaled down to monolayers, a direct energy bandgap emerges due to quantum confinement effects [2, 3]. WS_2 and MoS_2 monolayers are widely studied due to their unique optical [4, 5] and electronic [6] properties and potential applications in electronics and optoelectronics [7, 8].

MoS_2 probably is the most explored TMD. It can be synthesized in a form of powder, polycrystalline film, 2D nanosheets and nanotubes [9]. MoS_2 is an n-type semiconductor having the indirect and direct band gaps of E_{ig} = 1.2 eV and E_{dg} = 1.8 eV, respectively. MoS_2 is also chemically inert, thermally stable and not toxic [10].

Zinc oxide (ZnO) nanowires (NWs), that have been in focus of scientific community for decades, are still gaining increased attention due to the simplicity of synthesis and a number of beneficial properties. Among other applications, ZnO NWs can be used as a template for the synthesis of heterostructured nanomaterials [11]. Zinc oxide has two main phases: hexagonal wurtzite and cubic zincblende. Wurtzite is the most common and most stable structure, while zincblende form grows on substrates with cubic lattice structure. Bulk ZnO is known to be a direct band gap (3.2–3.3 eV) n-type semiconductor [12].

It is known that the use of core-shell materials with the shell having higher band gap leads to an enhancement of optical properties. Band gap of zinc sulfide (ZnS) for both zincblende (3.7 eV) and wurtzite (3.9 eV) forms is wider than that of ZnO at room temperature [13]. Therefore, ZnS is frequently used to improve luminescent properties of ZnO [14]. There are many methods to produce ZnS shell around ZnO core [15], and one of them is direct sulfidation process as it was demonstrated in [16].

Recently, several groups reported on wet chemical synthesis of ZnO-MoS_2 hybrid heterostructures [17, 18, 19]. In these studies, superior photocatalytic properties of ZnO-MoS_2 hybrid heterostructures were demonstrated, in particular for photocatalytic hydrogen evolution reaction and photodegradation of methylene blue and other organic dyes. Also direct coupling between ZnO nanorods and MoS_2 monolayers was used in [20] to enhance Raman and photoluminescence emission.

In this study we report for the first time on the synthesis of ZnO/ZnS/MoS_2 core-shell NWs by immersion of ZnO NWs in the solution of ammonium molybdate followed by annealing in

the sulfur atmosphere. Such ZnO/ZnS/MoS_2 core-shell nanostructures could potentially be applied for photocatalytic hydrogen evolution reaction and in dye-sensitized-like solar cells.

2. Experimental details.

ZnO/ZnS/MoS_2 core-shell nanowires were produced by a three-step route: 1) synthesis of ZnO NWs on a silicon wafer, 2) immersion of the ZnO NW sample in ammonium molybdate solution, 3) annealing of the sample in sulfur atmosphere.

ZnO NWs were grown by a chemical vapour transport method using spherical Au nanoparticles as a catalyst (Smart materials, water suspension, 50 nm in diameter) [10]. A 1:4 mixture of ZnO and graphite powders was heated to 900 °C in a quartz tube for 30 min in a stream of the carrier gas N_2. Nanowires were synthesized on an oxidized silicon wafers Si(100)/SiO_2 (Semiconductor Wafer, Inc.). At the next step, the samples were immersed into the solution of 0.125 g ammonium heptamolybdate $(NH_4)_6Mo_7O_{24}{\cdot}4H_2O$ in 20 ml H_2O and subsequently dried at room temperature. It is known that ammonium heptamolybdate decomposes at 350-400 °C with a formation of MoO_3 [21]. Therefore, finally, the samples were annealed in a quartz tube in the sulfur atmosphere during 0.5 hour at 700 °C to convert the molybdenum precursor (MoO_3) into MoS_2. Additional sample was prepared by annealing in the sulfur atmosphere during 0.5 hour at 500 °C to compare quality of MoS_2 shell at lower synthesis temperatures [22].

Morphology of pure ZnO and core-shell NWs on a silicon substrate was characterized by scanning electron microscopy (SEM, Lyra, Tescan). The inner crystalline structure of core-shell NWs was revealed using transmission electron microscopy (TEM, Tecnai GF20, FEI) operated at the accelerating voltage of 200 kV. The diffraction pattern was processed by CrysTBox software [23]. Confocal imaging and micro-Raman measurements were performed with confocal microscope with spectrometer Nanofinder-S (SOLAR TII). A diode pumped solid-state (DPSS) Nd:YAG laser (532 nm, max continuous wave (cw) power P_{ex} = 150 mW) was used as the excitation source. A Peltier-cooled back-thinned CCD camera (ProScan HS-101H) was used for

detection of Raman spectra. All measurements were performed in a back-scattering geometry through a Nikon CF Plan Apo 100× (NA = 0.95) optical objective.

2D MoS_2 nanosheets used as the reference sample were grown using a similar chemical vapour transport process in a quartz tube with a temperature gradient. Powders of MoO_3 (1 mg) and sulfur (0.25 g) were employed as solid sources: MoO_3 was heated to 700 °C and sulfur to 300 °C. Silicon substrate was placed downstream of precursors in the high-temperature zone (700 °C). At the end of the growth process, the furnace was let to cool down to the room temperature naturally. The gas flow rate was held constant throughout the procedure. The optimal growth parameters for the synthesis procedure of MoS_2 nanosheets were found to be 20 minutes at 700°C in the high-temperature zone.

Freshly grown MoS_2 nanosheets were studied by Eclipse L150 (Nikon) optical microscope; for higher resolution and contrast images SEM (Tescan, Vega II) was used. The thickness of prepared nanostructures was determined by atomic force microscope (AFM, CP-II, Veeco) in the tapping mode using PPP-NCHR probes with force constant 42 N/m and tip radius of curvature < 10 nm (Nanosensors).

3. Results and discussion.

SEM was used to control the growth of pure ZnO NWs and the change of their morphology after subsequent annealing in the sulfur atmosphere. It is clearly visible that the smooth surface of ZnO NWs, immersed in the ammonium heptamolybdate solution, (Fig. 1(a,b)) becomes significantly more rough and altered (Fig. 1(c,d)) after annealing.

Strong electrical charging was observed for the core-shell NWs, however was absent for pure ZnO NWs sample and sample immersed in the ammonium heptamolybdate solution. This may indicate that electrical properties of ZnO NWs were strongly affected by a shell layer, making them less conductive. It is known that sulfur reacts with ZnO at temperatures above 400 °C resulting in a formation of ZnS phase [16], which has the value of the bang gap (3.7 eV)

larger than ZnO (3.4 eV) [13]. Alternatively, MoS_2 shell may be responsible for electrical charging.

SEM images of 2D MoS_2 nanosheets with triangular and star shapes grown on Si(100)/SiO_2 wafer at 700 °C are shown in Fig. 1(e,f). These MoS_2 nanosheets were prepared as a reference sample for Raman spectroscopy.

TEM images of core-shell NWs annealed in sulfur atmosphere at 500 °C and 700 °C are shown in Fig. 2. Sample annealed at 500 °C has polycrystalline shell structure of zincblende ZnS, with remaining amorphous phase (Supplementary materials, Fig. S1). No MoS_2 shell was found around the NW, however few crystallites appearing as parallel black lines (Fig. 2(c)) may be identified as MoS_2.

It is easy to see that the shell is non-homogeneous and appears as a mosaic of dark and bright spots (Fig. 2(d,e)) or as microcrystals formed around the NW core (Fig. 2(g,h)) for the sample annealed at 700 °C. Analysis of selected area electron diffraction (SAED) image of a core-shell NW (Fig. 3) reveals the following phases: ZnO zincite (zone axis <0001>), ZnS zincblende (zone axis <001>), and MoS_2 molybdenite phases (zone axis <-2201> and <14-53>). Dominating (most intensive) diffraction spots belong to the ZnO core, while less intensive to ZnS and MoS_2 phases. Symmetric orientation of MoS_2 reflexes relative to ZnO reflexes may indicate epitaxial growth of MoS_2.

According to interplanar distance measurements and SAED analysis data, microcrystals on NW surface can be attributed to zincblende ZnS phase with the interplanar distance d=3.1-3.2 Å [16, 24]. Due to the lattice mismatch and different crystal structure of ZnO core and ZnS shell, the upper layer cannot grow as a smooth single crystal layer on top of ZnO NW surface.

We found that samples prepared at 700 °C are coated by a thin layer of MoS_2, which appears as a number of parallel black lines (MoS_2 monolayers) in Fig. 2(f,i). The number of MoS_2 layers varies in the range of 1-8 monolayers, which is probably related to nonhomogeneous coating by ammonium molybdate precursor. The measured distance between

monolayers is about 6.25 Å, which corresponds well to 6.2-6.3 Å interlayer distance in MoS_2 nanostructures [18, 25].

Alternatively, MoO_3 layer can be deposited on ZnO NWs by DC magnetron sputtering of Mo target in argon-oxygen atmosphere [26]. After sulfidation of ZnO-MoO_3 NWs at 700 °C, morphology of thus obtained core-shell NWs is rather similar to the ones produced by immersion in ammonium heptamolybdate solution (Supplementary materials, Fig. S2). However, MoS_2 shell is usually significantly thicker due to the large amount of deposited MoO_3 precursor (it is difficult to deposit very thin layer of MoO_3 by magnetron sputtering), therefore we can conclude that the immersion method of molybdenum precursor deposition is more preferable in such case compared to the magnetron sputtering.

In our previous work [27], no formation of detectable ZnS layer was observed after the synthesis of ZnO/WS_2 core-shell NWs at 800 °C, and ZnO core remained unaltered and single crystalline after the growth of WS_2 shell (Supplementary materials, Fig. S3). Worth noting that WS_2 growth starts on ZnO surface at the ZnO-WO_3 interface. Probably, WO_3 layer deposited by magnetron sputtering is able to protect ZnO core from sulfidation and/or WO_3 reaction with sulfur is more favourable than ZnO reaction with sulfur.

The phase composition of individual nano-objects such as NWs and 2D nanosheets can be probed by micro-Raman spectroscopy. The results for two samples, a NW and a 2D MoS_2 nanosheet, are reported in Fig. 4. Note that the thickness of the 2D MoS_2 reference nanosheet, measured by AFM, is about 2.6 nm that corresponds to approximately 4 monolayers [28].

The obtained Raman spectrum of the core-shell NW (Fig. 4(d)) is similar to that of the 2D MoS_2 nanosheet (Fig. 4(b)), which confirms the formation of MoS_2 layer on the NWs. The in-plane E^1_{2g} mode at 384 cm^{-1} and the out-of-plane A_{1g} mode at 407 cm^{-1} were clearly resolved on the 2D MoS_2 nanosheet (Fig. 4(b)). The same modes E^1_{2g} at 384 cm^{-1} and A_{1g} at 407 cm^{-1} were observed on the core-shell NW (Fig. 4(c,d)). [29, 30]. Note that the large peak at ~521 cm^{-1} is the

first order of optical mode at k=0 of the underlying silicon substrate [31]. No Raman bands due to ZnO [32] and ZnS [33] phases were observed because of their weak Raman activity.

4. Conclusions.

In this study we demonstrated a simple process for the production of core-shell ZnO/ZnS/MoS_2 nanowires. A few-layer MoS_2 shell was grown on ZnO NW core by immersing ZnO NWs in ammonium molybdate solution, followed by annealing in a sulfur atmosphere at 700 ºC. Two solid state chemical reactions occur during the annealing and result in a formation of ZnS and MoS_2 layers. The annealing at lower temperature (500 ºC) is not sufficient for a formation of continuous MoS_2 shell. Morphology and internal structure of the synthesized ZnO/ZnS/MoS_2 core-shell NWs were investigated by SEM and TEM, respectively. The formation of zincblende ZnS interlayer and MoS_2 shell was confirmed by SAED analysis and micro-Raman spectroscopy, respectively.

Acknowledgements

The present research was supported by the Latvian National Research Program IMIS2. Authors are grateful for Dr. Robert Kalendarev and Martins Zubkins for assistance in magnetron sputtering, Dr. Krisjanis Smits for TEM measurements, Dr. Roberts Zabels for AFM measurements and Reinis Ignatans for XRD measurements.

5. REFERENCES

[1] P. Hajiyev, C. X. Cong, C. Y. Qiu, T. Yu, Contrast and Raman spectroscopy study of single-and few-layered charge density wave material: 2H-$TaSe_2$, Sci. Rep. 3 (2013) 2593.

[2] A. Splendiani, L. Sun, Y. Zhang, T. Li, J. Kim, C. Y. Chim, F. Wang, Emerging photoluminescence in monolayer MoS_2, Nano Letters 10 (4) (2010) 1271–1275.

[3] G. L. Frey, R. Tenne, M. J. Matthews, M. S. Dresselhaus, G. Dresselhaus, Optical properties of MS_2 (M = Mo, W) inorganic fullerene-like and nanotube material optical absorption and resonance Raman measurements, J. Mater. Res. 13 (1998) 2412−2417.

[4] C. Ballif, M. Regula, P. E. Schmid, M. Remškar, R. Sanjinés, F. Lévy, Preparation and characterization of highly oriented, photoconducting WS_2 thin films, Appl. Phys. A-Mater. 62 (1996) 543.

[5] K. F. Mak, C. Lee, J. Hone, J. Shan, T. F. Heinz, Atomically thin MoS_2: a new direct-gap semiconductor, Phys. Rev. Lett. 105 (2010) 136805.

[6] G. Eda, H. Yamaguchi, D. Voiry, T. Fujita, M. Chen, M. Chhowalla, Single-layer MoS_2 transistors, Nano Lett. 11 (2011) 5111.

[7] G. Eda and S. A. Maier, Two-Dimensional Crystals: Managing Light for Optoelectronics, ACS Nano 7 (2013) 5660–5665.

[8] D. Xiao, G. B. Liu, W. X. Feng, X. D. Xu, W. Yao, Coupled spin and valley physics in monolayers of MoS_2 and other group-VI dichalcogenides, Phys. Rev. Lett. 108 (2012) 196802.

[9] I. Song, C. Park, H. C. Choi, Synthesis and properties of molybdenum disulphide: from bulk to atomic layers, RSC Adv. 5 (2015) 7495–7514.

[10] N. Wang, F. Wei, Y. Qi, H. Li, X. Lu, G. Zhao, Q. Xu, Synthesis of Strongly Fluorescent Molybdenum Disulfide Nanosheets for Cell-targeted Labelling ACS Appl. Mater. Interfaces 6 (22) (2014) 19888–19894.

[11] H.-Y. Liu, Z.-B. Feng, J. Wang, J.-Y. Diao, D.-S. Su, Synthesis of hollow carbon nanostructures using a ZnO template method, New Carbon Mater. 31(1) (2016) 87-91.

[12] U. Ozgur, Y. I. Alivov, C. Liu, A. Teke, M. A. Reshchikov, S. Doğanc, V. Avrutin, S.-J. Cho, H. Morkoc, A comprehensive review of ZnO materials and devices, J. Appl. Phys. 98 (2005) 041301.

[13] Safa Kasap, Peter Capper (Eds.), Handbook of Electronic and Photonic materials, Springer US, 2007. 2 (Chapter 16).

[14] Y. Ding, X. D. Wang, Z. L. Wang, Phase controlled synthesis of ZnS nanobelts: zinc blende vs wurtzite, Chem. Phys. Lett. 398 (2004) 32–36.

[15] J. Li, D. Zhao, X. Meng, Z. Zhang, J. Zhang, D. Shen, Y. Lu, X. Fan, Enhanced Ultraviolet Emission from ZnS-Coated ZnO Nanowires Fabricated by Self-Assembling Method, J. Phys. Chem. B. 110 (2006) 14685-14687.

[16] S. K. Panda, A. Dev, and S. Chaudhuri, Fabrication and Luminescent Properties of c-Axis Oriented ZnO-ZnS Core-Shell and ZnS Nanorod Arrays by Sulfidation of Aligned ZnO Nanorod Arrays, J. Phys. Chem. C. 111, (2007) 5039-5043.

[17] Y.-J. Yuan, F. Wang, B. Hu, H.-W. Lu, Z.-T. Yu, Z.-G. Zou, Significant Enhancement in Photocatalytic Hydrogen Evolution from Water by MoS_2 Nanosheet-coated ZnO Heterostructure Photocatalyst, Dalton Transactions, 44, (2015) 10997-11003.

[18] Y.-H. Tan, K. Yu, J.-Z. Li, H. Fu, Z.-Q. Zhu, MoS_2@ZnO nano-heterojunctions with enhanced photocatalysis and field emission properties, J. Appl. Phys. 116 (2014) 064305.

[19] Y. Liu, S. Xie, H.Li, X. Wang, A Highly Efficient Sunlight Driven ZnO Nanosheet Photocatalyst: Synergetic Effect of P-Doping and MoS_2 Atomic Layer Loading, Chem. Cat. Chem., 6 (2014) 2522 – 2526.

[20] K. Zhang, Y. Zhang, T. Zhang, W. Dong, T. Wei, Y. Sun, X. Chen, G. Shen, N. Dai, Vertically coupling ZnO nanorods on MoS_2 monolayers with enhanced Raman and photoluminescence emission, Nano Research 8(3) (2015) 743–750.

[21] X. W. Lou, H. C. Zeng, Hydrothermal Synthesis of r-MoO_3 Nanorods via Acidification of Ammonium Heptamolybdate Tetrahydrate, Chem. Mater. 14 (2002) 4781-4789.

[22] L. Zhang, C. Liu, A. B. Wong, J. Resasco, P. Yang, MoS2-wrapped silicon nanowires for photoelectrochemical water reduction. Nano Research, 8 (2015) 281–287.

[23] M. Klinger, A. Jäger, Crystallographic Tool Box (CrysTBox): automated tools for transmission electron microscopists and crystallographers, J. Appl. Crystallogr., 48 (2015) 2012-2018.

[24] D. Jiang, L. Cao, W. Liu, G. Su, H. Qu, Y. Sun, B. Dong, Synthesis and Luminescence Properties of Core/Shell ZnS:Mn/ZnO Nanoparticles, Nanoscale Res. Lett. 4 (2009) 78–83.

[25] R. Francis, L. Deepak, A. Mayoral, A. J. Steveson, S. Mejıa-Rosales, D. A. Blomd, M. Jose-Yacaman, Insights into the capping and structure of MoS_2 nanotubes as revealed by aberration-corrected STEM R, Nanoscale 2 (2010) 2286–2293.

[26] J. Purans, A. Kuzmin, P. Parent, C. Laffon, X-ray absorbtion study of the electronic structure of tungsten and molybdenum oxides on the O K-edge, Electrochimica Acta 46 (2001) 1973-1976.

[27] B. Polyakov, A. Kuzmin, K. Smits, J. Zideluns, E. Butanovs, J. Butikova, S. Vlassov, S. Piskunov, Yuri F Zhukovskiiy, Unexpected Epitaxial Growth of Few WS_2 Layers on {1-100} Facets of ZnO Nanowires, J. Phys. Chem. C. 120 (2016) 21451−21459.

[28] Y.-H. Lee, X.-Q. Zhang, W. Zhang, M.-T. Chang, C.-T. Lin, K.-D. Chang, Y.-C. Yu, J. T.-W. Wang, C.-S. Chang, L.-J. Li, T.-W. Lin, Synthesis of Large-Area MoS_2 Atomic Layers with Chemical Vapor Deposition, Adv. Mater. 24 (2012) 2320–2325.

[29] A. L. Elias, N. Perea-Lopez, A. Castro-Beltran, A. Berkdemir, S. Feng, M. Terrones, Controlled synthesis and transfer of large-area WS_2 sheets: From single layer to few layers, ACS Nano. 7(6) (2013) 5235–5242.

[30] P. Tonndorf, R. Schmidt, P. Bottger, X. Zhang, Photoluminescence emission and Raman response of monolayer MoS_2, $MoSe_2$ and WSe_2, Optics Express. 21(4) (2013) 4908-4916.

[31] J. H. Parker, D. W. Feldman, M. Ashkin, Raman scattering by silicon and germanium, Phys. Rev., 155 (1967) 712-714.

[32] K.A. Alim, V.A. Fonoberov, M. Shamsa, A. A. Balandina, Micro-Raman investigation of optical phonons in ZnO nanocrystals, J. Appl. Phys. 97 (2005) 124313.

[33] Y. C. Cheng, C. Q. Jin, F. Gao, X. L. Wu, W. Zhong, S. H. Li, P. K. Chu, Raman scattering study of zinc blende and wurtzite ZnS, J. Appl. Phys. 106 (2009) 123505.

Figure 1. SEM images of ZnO NWs, immersed in ammonium heptamolybdate solution and dried (a,b); core-shell ZnO/ZnS/MoS_2 NWs after annealing in sulfur atmosphere at 700°C (c,d); 2D MoS_2 nanosheets grown on a silicon wafer at 700°C (e,f).

Figure 2. TEM images of core-shell NWs annealed in sulfur atmosphere at 500°C (a-c) and 700°C (d-i). Layers of MoS_2 are visible as black lines on top of the NWs surface (f, i).

Figure 3. SAED analysis of core-shell NWs annealed in sulfur atmosphere at 700 °C. The presence of ZnO zincite zone axis <0001> (a,b), ZnS zincblende zone axis <001> (c,d), and MoS_2 molybdenite phases of zone axis <-2201> (e,f) and zone axis <14-53> (g,h) were identified.

Figure 4. AFM image (a) and micro-Raman spectrum (b) of 2D MoS_2 nanosheet on a silicon substrate. Confocal microscope image of ZnO/ZnS/MoS_2 NW on a silicon substrate (c) and the corresponding micro-Raman spectrum (d).

Figures

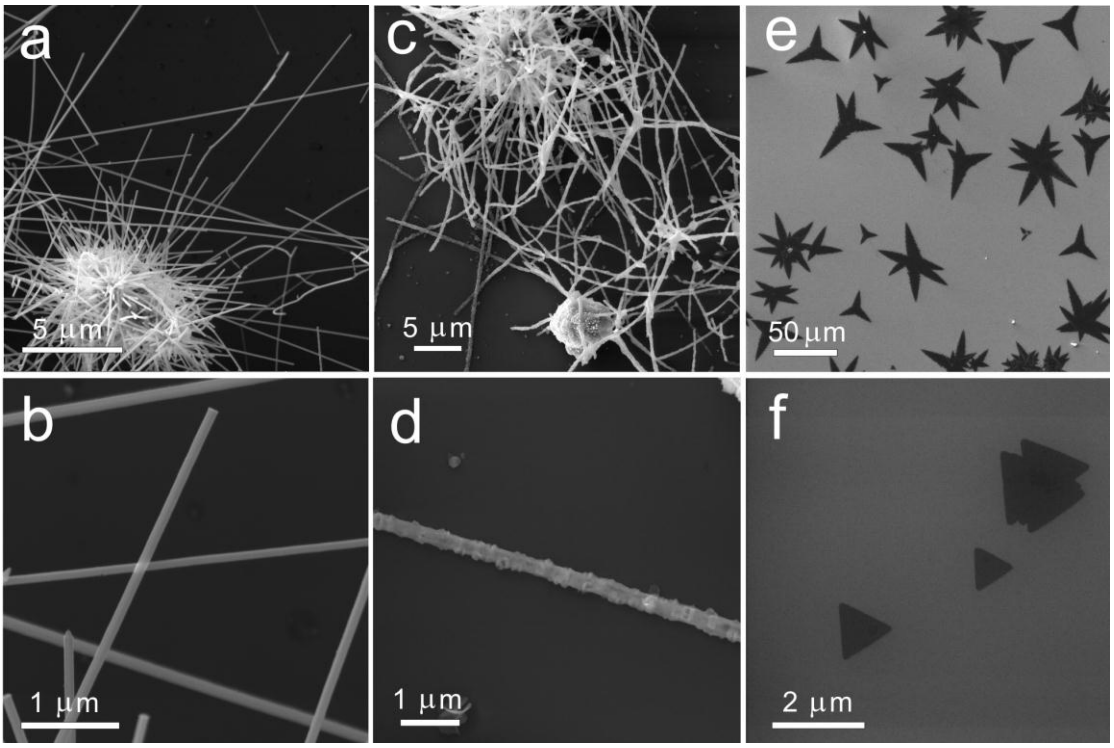

Figure 1.

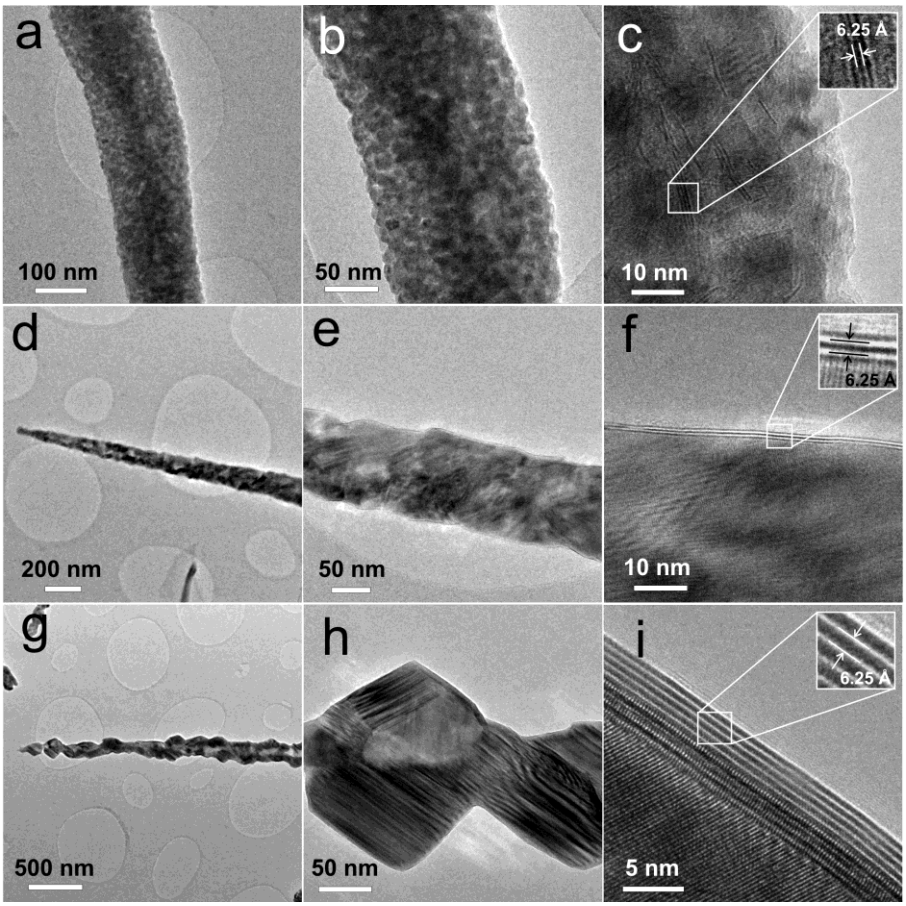

Figure 2.

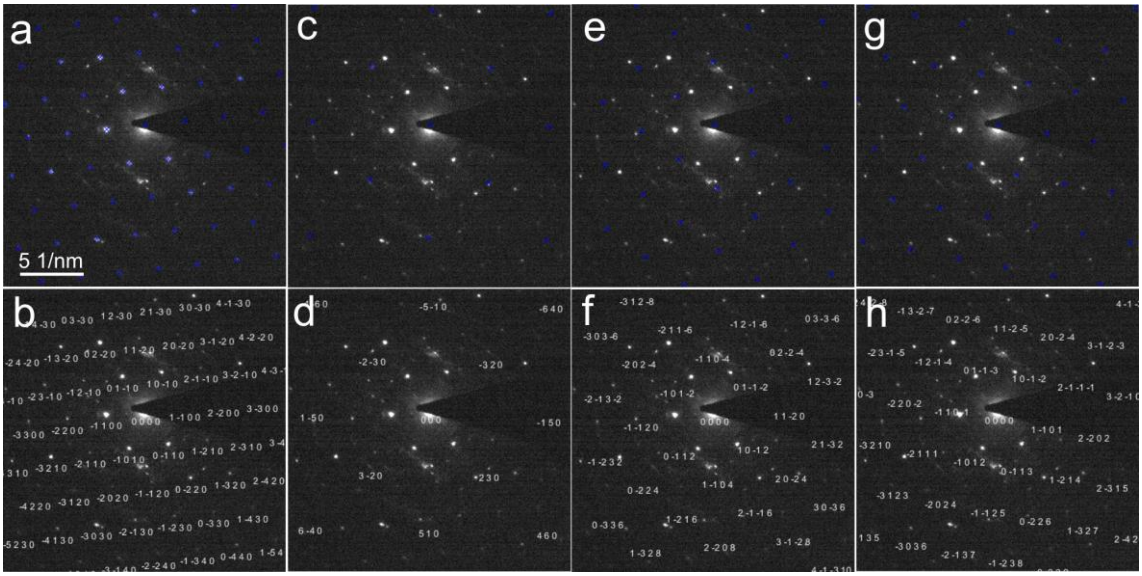

Figure 3.

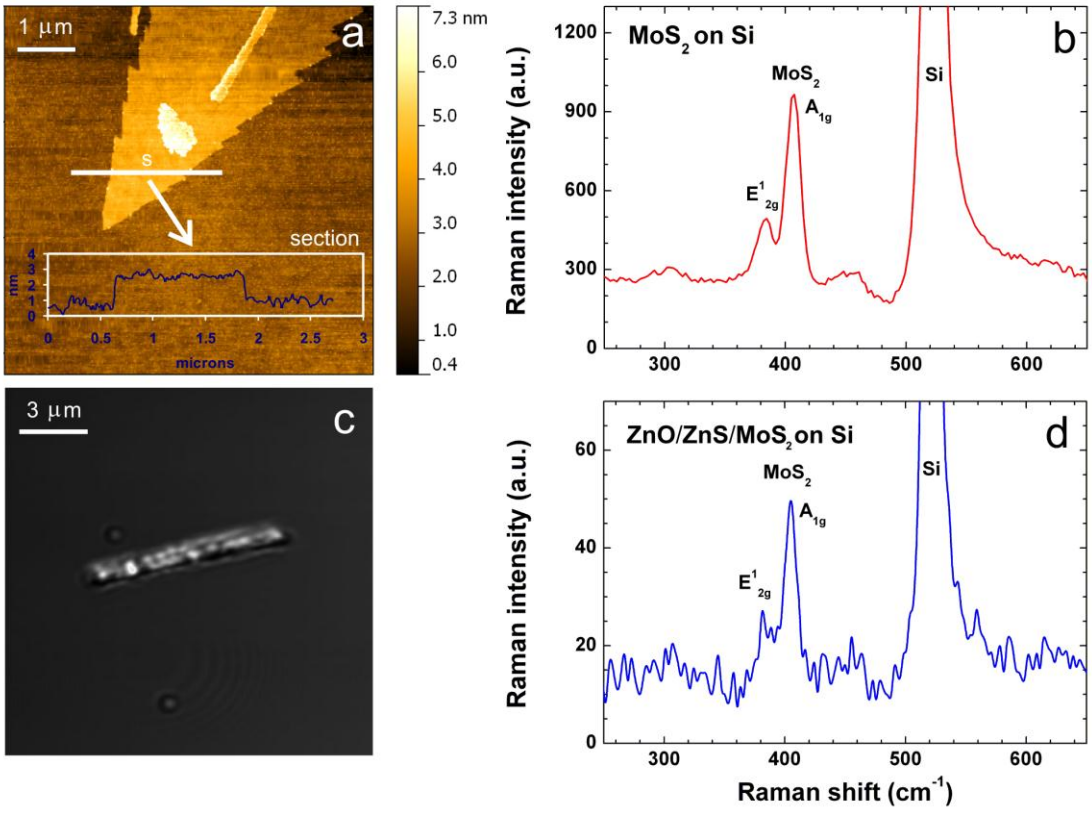

Figure 4.

Highlights

- A novel synthesis strategy of ZnO/ZnS/MoS_2 core-shell nanowire growth is described.
- A formation of zincblende ZnS interlayer is confirmed by SAED analysis.
- A formation of MoS_2 layers is confirmed by SAED analysis and Raman spectroscopy.

Institute of Solid State Physics, University of Latvia as the Center of Excellence has received funding from the European Union's Horizon 2020 Framework Programme H2020-WIDESPREAD-01-2016-2017-TeamingPhase2 under grant agreement No. 739508, project CAMART²